3 Search for μ-e Conversion with SINDRUM II

Andries van der Schaaf

in collaboration with: Willi Bertl, PSI

The measurements discussed here were performed in the year 2000 by: W. Bertl, F. Rosenbaum and N.M. Ryskulov, Paul Scherrer Institute, R. Engfer, E.A. Hermes, G. Kurz, A. van der Schaaf and P. Wintz, Physik-Institut der Universität Zürich, J. Kuth and G. Otter, RWTH Aachen, and T. Kozlowski and I. Zychor, IPJ Swierk.

(SINDRUM II Collaboration)

3.1 Data taking stopped

In the year 2000 SINDRUM II raised the sensitivity to neutrino-less μ-e conversion on heavy targets by two orders of magnitude. In a preliminary analysis [1] no signal was observed and since no further large improvements in sensitivity can be expected the experiment was stopped.

In the past year the two of us left to finish the project have focused on a better understanding of the observed electron distribution which has a dominant contribution from μ^- decay in orbit (MIO). Other sources of electrons, such as radiative muon capture followed by $\gamma \rightarrow e^+e^-$ or μ^- decay in flight, have contributions of $O(\%)$ which can be ignored. Once a good description of the observed distributions has been obtained a reliable estimate can be made of the new limit on μ-e conversion on gold.

3.2 High-momentum component of decay electrons from muonic gold

The energy distribution of electrons from the decay of free muons at rest peaks at the kinematic endpoint $m_\mu c^2/2$. In muonic atoms the endpoint is raised to $m_\mu c^2 - B - R$, with B: μ^- binding energy and R: nuclear recoil energy. The energy distribution has been calculated for various cases. We use results for lead [2] correcting for the 0.54 MeV shift in endpoint energy. The resulting spectrum is shown in Fig.3.1.

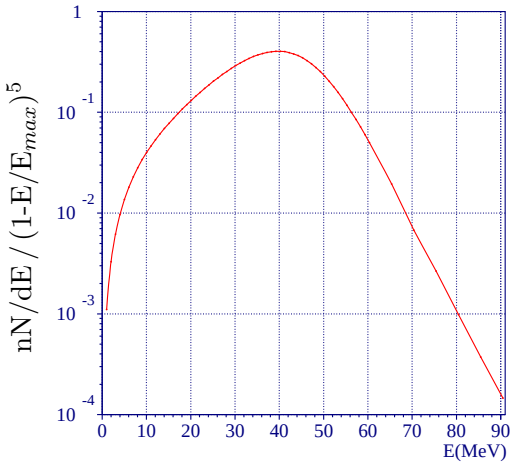

Figure 3.1: *Theoretical energy distribution weighed by 1/(1-E/E_{max})^5 for electrons from the decay of muonic gold. Note the linear energy dependence above 60 MeV resulting from the weighting. The yield per stopped muon drops to* 5.15×10^{-7}, 5.67×10^{-8} *and* 4.36×10^{-9} *for energy thresholds of 70, 75 and 80 MeV, respectively.*

Detailed studies were made of:

- *the number of muon stops*

  The number of muons stopping in the target was measured during the experiment by observing the characteristic muonic gold X-rays penetrating the superconducting coil

of the spectrometer (see figures 3.2 and 3.3). The sensitivity of the monitor was determined by simulation and reproduced with an accuracy of 3 % by a calibration using ^{137}Cs and ^{60}Co sources. The number of muons stopping during the live time of the experiment was determined as:
$N_\mu^{stop} = (4.30 \pm 0.3_{stat} \pm 0.3_{sys}) \times 10^{13}$.

- *exact geometry of the spectrometer.*

  Careful adjustments were made of the parameters in the simulation that describe the relative positions of the various detector components and vacuum flanges.

- *position of the two gold tubes used as stopping target* and *the distribution of muon stops over the target.*

  As can be seen from the distributions of Fig. 3.4 the target was off centre by more than a centimetre which has a strong effect on the acceptance of the spectrometer at the low end of the observed energy distribution. Better knowledge of the target geometry also allows a better suppression of backgrounds from cosmic rays and reconstruction errors.

- *variations of the tracking efficiency during data taking.*

  Tracks in the main drift chamber have typically thirty anode hits and roughly half of them have cathode information as well. During the measurements this single-hit cathode efficiency varied within a factor two, however, depending on parameters such as gas quality and chamber high voltage.

- *precision of the tracking detector.*

  The observed position resolution versus drift time was implemented in the event simulation.

- *the efficiency of the Cerenkov end-cap detector.*

  For a correct description of the observed distribution of polar angle it is crucial to account for the angular dependence of the light collection efficiency.

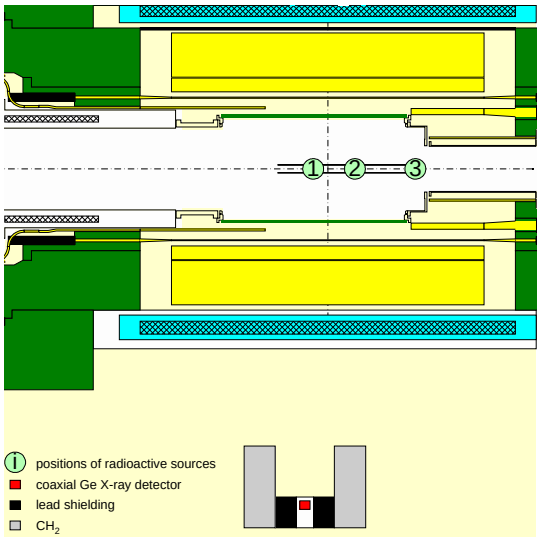

Figure 3.2: *Horizontal cross-section through the spectrometer showing the location of the X-ray monitor.*

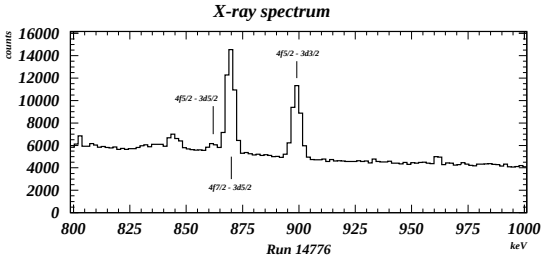

Figure 3.3: *X-ray spectrum accumulated during 3 hours of μe data taking.*

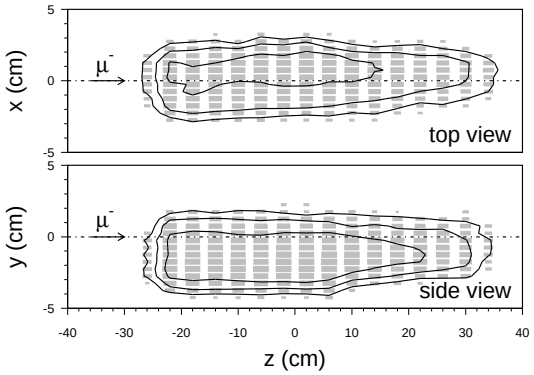

Figure 3.4: *Distributions of the trajectory's point of closest approach to the spectrometer axis. The target consisted of two tubes of 32 cm length each. As can be seen the downstream target had a slightly smaller diameter (38 mm, as compared to 45 mm for the upstream tube).*

- *calibration of the field/current relation.*

  The momentum calibration is done with the endpoint of the *Michel* decay $\mu^+ \to e^+\nu\overline{\nu}$ taken with scaled and reversed spectrometer field. Since there appears to be an offset in the setting of the power supply we measured the scaling factor directly with a Hall probe.

- *the inhomogeneity of the magnetic field*

  The spectrometer field drops by $\approx 10\%$ towards the downstream end of the tracking region. Ten years ago the field was precisely mapped and the observed distribution is taken into account in the momentum fit. Recent changes in the downstream mirror plate led to further distortions in the field shape. We determined their effect on the momentum calibration by studying the endpoint of the $\mu^+ \to e^+\nu\overline{\nu}$ decay versus polar angle. Figure 3.5 shows the resulting spectrum, which is in perfect agreement with the expectations from the event simulation.

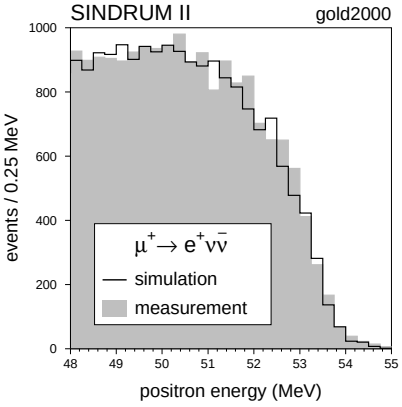

Figure 3.5: *Positron energy distributions for μ^+ beam and scaled spectrometer field.*

Figure 3.6 compares the measured energy and angle distributions with the predictions from the GEANT simulation. The shape of the stop distribution along the target was adjusted. The agreement is quite satisfactory given the 10-20% errors introduced by uncertainties in quantities such as the number of stopped muons, the value of the magnetic field, the shape of the beam profile, the trigger and selection efficiencies. The structure in the φ distribution reflects the shift in the target position. The dip around $\theta = 90^o$ is caused by the endcap requirement. The drop of the event rate towards lower energies is caused by the lower threshold on tranverse momentum resulting from the cylindrical symmetry of the spectrometer. The overall efficiency varies as a function of electron energy: from $\approx 1\%$ around 75 MeV where the event rate has its maximum to $\approx 10\%$ in the region of interest for μe conversion. As a next step we will focus on that region.

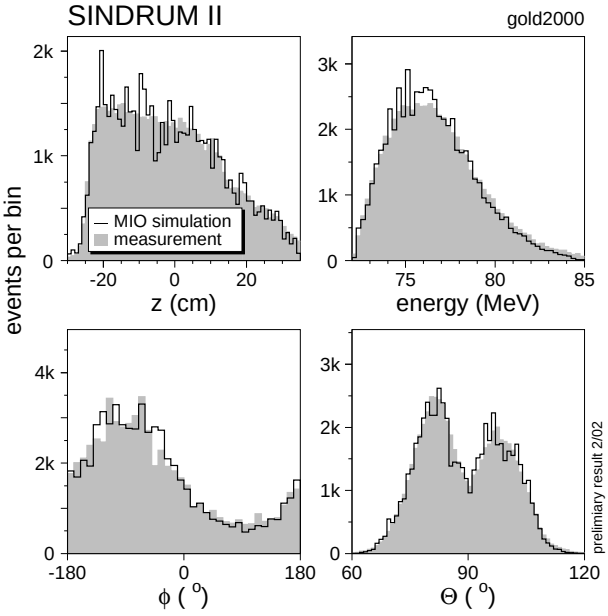

Figure 3.6: *Comparison of measurement and simulation of muon decay in orbit for various kinematic quantities.*

References

[1] SINDRUM II Collab., Annual Report 2000-2001, Physik-Institut, Zurich University.

[2] R. Watanabe *et al.*, Atom. Data and Nucl. Data Tab. **54** (1993), 165.